Method and Theory in Physical Organic Chemistry

Contributors

T. I. Danilenko
I. Golovata
K. Z. Gumargalieva
E. V. Kalugina
V. A. Korotkikh
Yu. A. Mikheev
A. I. Rakhimov
O. Romanyuk
N. A. Storozhakova
A. Turovskiy
E. Zagladko
[illegible]. Zaikov
[illegible]. Kozlov
[illegible]. Zaikov

Gennady E. Zaikov
Vadim G. Zaikov
(Editors)

NOVA

METHOD AND THEORY IN PHYSICAL ORGANIC CHEMISTRY

GENNADY E. ZAIKOV
AND
VADIM G. ZAIKOV
EDITORS

For permission to use material from this book please contact us:
Telephone 631-231-7269; Fax 631-231-8175
Web Site: http://www.novapublishers.com

Library of Congress Cataloging-in-Publication Data

Method and theory in physical organic chemistry / Gennady E. Zaikov and Vadim G. Zaikov, editors.
p. cm.
Includes bibliographical references and index.
ISBN 1-59454-401-8
1. Chemistry, Physical organic. I. Zaikov, Gennadiæi Efremovich. II. Zaikov, Vadim G.
QD476.M476 2005
547'.1--dc22 2005008891

Published by Nova Science Publishers, Inc. ✦ New York

METHOD AND THEORY IN PHYSICAL ORGANIC CHEMISTRY

PREFACE

The farer the experiment is from the theory,
The closer it is to the Nobel Prize
Frederic J. Curie
France, XX century

A man is blissful knowing nothing.
He will not be misunderstood.
Confucius
The Ancient China

Aristoteles asserted that 'among the unknown in the nature surrounding us the most unknown thing is time, because nobody knows, what time is and how it can be controlled'. Since then definite positive changed happened in this field. Particularly, the branch of science named chemical kinetics was established, which gives an opportunity to predict behavior of chemical reagents with time and disclose the inner mechanism of the interaction between particles (molecules, ions, radicals and atoms) in various chemical processes.

This Collection is devoted in general to chemical kinetics as a tool, which helps in understanding the process mechanism and, consequently, gives an opportunity to forecast behavior of molecules and their fragments, and control the process. It includes articles on polymer degradation and stabilization, polymerization processes, the study of specific solid and liquid reactions from positions of chemical kinetics, quantum-chemical calculations in chemical reactions, the role of transition metals in aging and stabilization of polymers, regulation of thermal conditions under fast chemical reactions, the study of the properties and practicing of plastics, natural and synthetic rubbers, and the features of liquid phase structure.

Dr. Vadim G. Zaikov and Prof. Gennady E. Zaikov
N.M. Emanuel Institute of Biochemical Physics
Russian Academy of Sciences
4 Kosygin str., Moscow 119991, Russia

CONTENTS

In: Method and Theory in Physical Organic Chemistry
Editors.: V. G. Zaikov and G. E. Zaikov, pp. 1-43
ISBN 1-59454-401-8

Chapter 1

DEGRADATION OF POLYSULFONES AND POLYESTERIMIDES

E. V. Kalugina
Polyplastic Co., 14A, General Dorokhov st., Moscow 119530, Russia
K. Z. Gumargalieva
N.N. Semenov Institute of Chemical Physics, 4, Kosygin st., Moscow 119991, Russia
G. E. Zaikov
N.M. Emanuel Institute of Biochemical Physics, 4, Kosygin st., Moscow 119991, Russia

DEGRADATION IN MELT

Polysulfones

Thermal analysis at programmed temperature increase, starting from 390 - 420°C, displays the beginning of mass losses of the most well-known polysulfone (PSF) derived from dichlorodiphenilsulfone and bisphenol A. Intensive PSF degradation, initiated at 5°/min heating rate, is ended at 650°C forming no coke residues. A slight bending on TGA curve at 550°C and 50% mass loss indicates process proceeding seemingly in two stages. At the initial stage of the process, effective constants of mass losses in the presence and in the absence of oxygen (in pure argon flow) equal

$$K_{O_2} = 4.3 \times 10^7 \exp\left(-\frac{92 \pm 20}{RT}\right), \text{min}^{-1},$$

and

$$K_{Ar} = 2.4 \times 10^{13} \exp\left(-\frac{190 \pm 20}{RT}\right), \text{min}^{-1},$$

respectively. In this case, oxygen effect is displayed not by gross rates of initial PSF degradation which obeys the order one kinetic law, but exothermal DTA peak initiated at 400°C typical of thermal oxidation and the presence of 30 wt.% coke residue at purely thermal process.

Mass loss is a low-sensitive parameter of PSF degradation during processing. For example, at 320°C PSF mass is stable during 0.5 h. Only 4 h after the losses reach about 2 wt.%. Color and molecular-mass parameters of PSF are sensitive to high-temperature degradation. Let us limit current discussion of PSF high-temperature degradation by processing temperature interval and temperatures approaching it and observed in the processing because of some deviations from the procedure. Therefore, temperature range to be considered is 280 - 350°C. Processing duration, including alerts, is about 1 h, mostly 10 - 30 min. Degradation changes in the mentioned exposures are noticeable, but kinetics of these changes is not clear enough. To clarify the mechanism of high-temperature degradation, the authors extended the observation period to 10 h, which allowed detection of the kinetic features of the process and basic chemical changes in the polymer.

Degradation changes in blocked PSF with the minimal concentration of additives are low in the mentioned temperature range without O_2. For example, as the sample is heated at 320°C in vacuum during 2 h, its light transmittance (λ = 425 nm, in solution) decreases from 98 to 95%. Index M_z, most sensitive to degradation, increases by 2 thousand, which is comparable with the measurement accuracy. Pure thermal transformation in PSF samples with non-optimal content of labile structures and additives are noticeable: heating at 320°C during 2 h may reduce light transmittance by 20 – 30 units and increase M_z by 10,000 – 20,000. Laboratory tests confirm analysis of samplings from real PSF production. Relatively short-term thermal impact (10 – 20 min at 300 - 320°C with respect to location in laminar flow) without air access reduces light transmittance by 5 – 7 units and increases M_z by 10,000. Let us accept that in the absence of oxygen PSF is stable in the processing temperature range.

Processing simulation on IIRT device at temperature below 300°C does not affect PSF. Though 1 h exposure at 300°C causes no effect on MFI, changes in molecular-mass parameters and coloring indicate PSF degradation (Figure 1). Kinetics of PSF coloring under thermal impact remain unchanged with temperature (order one law), effective activation energy equals (88 ± 15) kJ/mol in the temperature range of 280 - 350°C. Curves of molecular parameter changes are of more complicated shape. Thermal impact at 300°C increases all MMD moments, though this increase is low and does not affect MFI. At high temperatures powder-like sample tests indicate simultaneous increase of MFI and MMD moments. This is nontrivial rheological fact, because MFI is inversely related to molecular characteristics. Possible effects associated with powder melting and melt formation are not discussed in this monograph. Here we only note the initial tendency to molecular mass increase and not yet understandable MFI increase.

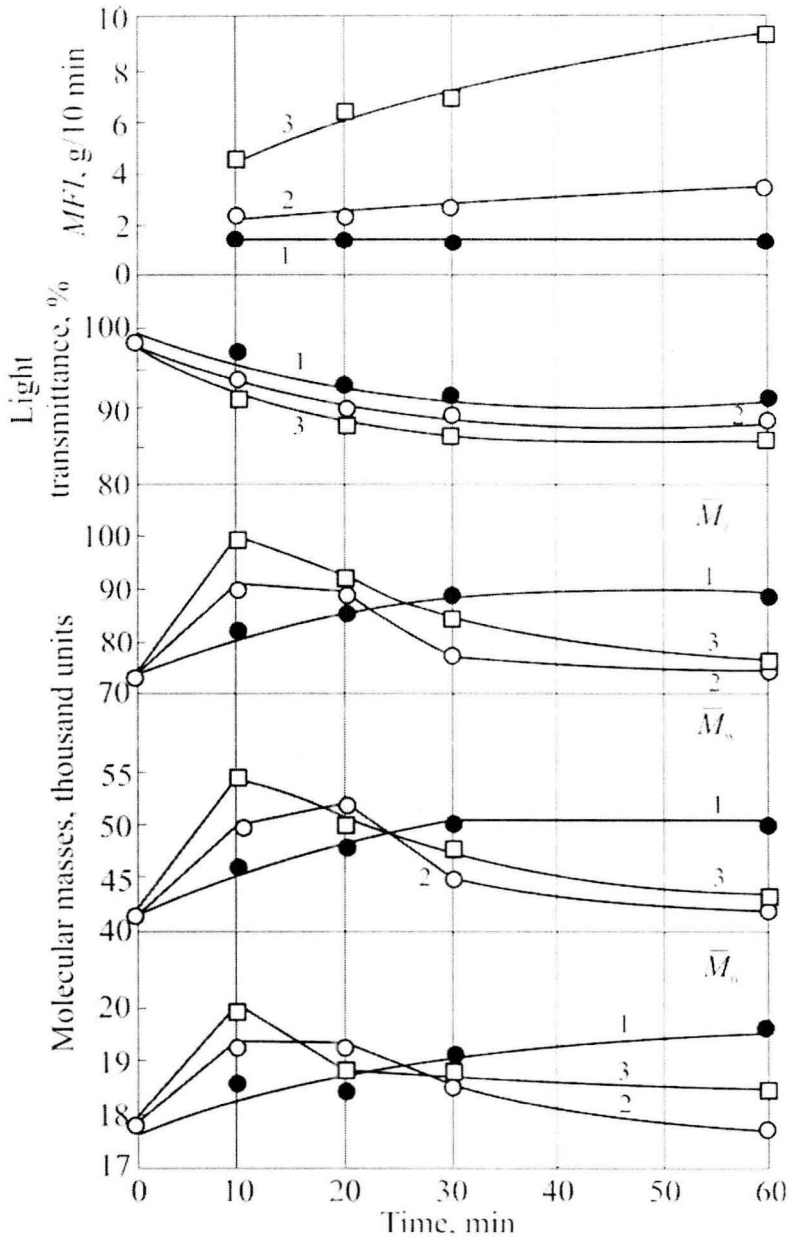

Figure 1. The effect of thermal processing on IIRT device (load 2.16 kg) on MFI, light transmittance, molecular-mass characteristics (M_z, M_w, M_n) of PSF at 300°C (1), 320°C (2) and 350°C (3)

Two reasons of these effects are possible: mechanical degradation caused by shift stresses in the channel and thermal oxidation by O_2 dissolved in the polymer. The first factor is altered in the experiment by varying the load, and the second is uncontrollable in tests on IIRT device.

Changes of PSF molecular characteristics and coloring were estimated by standard procedures of MFI determination with 2.16 and 21.6 kg loads in accordance with the following formula [1]:

$$\tau_n = \frac{Mgr}{2\pi R^2 (z + mr)},$$

where τ_n is the shear stress at IIRT channel wall; M is the load (in kg); g is acceleration of gravity; r is the capillary radius (in mm); R is the cylinder radius (in mm); m is a constant equal 2; z is the capillary length (in mm). In the present case, τ_n equals 1.3×10^5 dyn/cm^2. For comparison purposes a sample was estimated subject to analogous thermal impact (320°C, τ_n = 0) at P_{O_2} = 26.6 kPa. Difference in light transmittance of these three samples equals 1 – 2 units. M_w and M_n values differ by 500 – 1,000 that falls within the experiment accuracy, and only M_z moment increases by 5,000 – 6,000 with the shear stress. Let us assess the shear stress for real processing equipment, for example, at the wall in single-screw extruder [1]:

$$\tau_n = \eta\gamma_w,$$

where η is PSF melt viscosity; γ_w is the melt shear rate at the wall; η is determined from MFI: for PSF $\eta = 5\times10^4\ G\rho/\mathrm{MFI}$ at the load G = 2.16 kgf and density ρ = 1.24 g/cm^2, and MFI of serial lots with the average 5 g/10 min MFI, $\eta = 2.7\times10^5$ dyn·s/cm^2. As $\gamma_w = 20$ s^{-1}, $\tau_n = 5.4\times10^6$ dyn/cm^2.

Thus, according to shear stresses determined, mechanical loads on PSF macromolecules at processing in the most rigid mode on IIRT device (maximal load is 21.6 kgf) are almost identical. Therefore, whenever in tests on IIRT device with τ_n changes by an order of magnitude mechanical degradation was low even on the background of spontaneously degrading sample (τ_n = 0), further 3 – 5 time increase of τ_n at transition to processing equipment may hardly cause a sharp intensification of mechanical degradation. Actually, vacuum-extrusion (residual pressure equals 20 – 50 mmHg) of powder-like PSF increased just insignificantly the degradation effects detected in tests on IIRT device. Thus, thermal effect in the presence of oxygen causes degradation changes in PSF. Mechanical impact applied in the form of loads corresponded to processing conditions specifically increases degradation. However, this effect is negligibly lower compared with the presence of oxygen, which increases M_w and M_n to 2,000 – 5,000, and M_z to 10,000 or higher. Mechanical loads do not affect coloring, which change is typical feature of high-temperature PSF degradation during processing.

The following fundamental fact should be noted: the main contribution to degradation changes in PSF under processing conditions and in processing temperature range is associated with the presence of oxygen in the system. The next stage of investigations will determine PSF and O_2 interaction features at high temperatures. Since mechanical loads under current conditions have an insignificant effect on the degradation process, and the atmosphere monitoring in processing equipment is difficult or impossible, high-temperature degradation of PSF in the presence of oxygen was studied on freely disposed sample.

As heated in melt, PSF quickly absorbs oxygen and releases CO_2 (Figure 2), water and formaldehyde that clearly indicates the oxidation type of interaction between PSF macromolecules and O_2. Kinetic curves of O_2 absorption are shaped identically at temperatures below 350°C and O_2 partial pressure corresponded to its concentration in air: the induction period is absent and two parts are clearly observed. The initial part is 2 – 3 h long

and is characterized by high rates. The second part displays gradual decrease of the process rate with transition to linear process, traced up to 10 h exposure. The effective activation energy calculated from initial rates of O_2 absorption in the temperature range of 280 - 350°C equals (72 ± 12) kJ/mol. This E_a value for high-temperature oxidation is close to other arylaliphatic polymers - polyalkanimide (57 kJ/mol) and aliphatic-aromatic polyamides (52 - 54 kJ/mol), described in [1] and [2]. Hence, this value drastically differs from $E_a \approx 0$ of PE high-temperature oxidation in the same temperature range [3, p. 103]. The second stage of PSF oxidation is almost independent of temperature - E_a = 11 kJ/mol, and by this parameter PSF oxidation in melt at deep stages is similar to PE behavior.

Semi-logarithmic anamorphism of time dependences of the O_2 absorption rate at PSF heating in melt (Figure 3) with respect to O_2 pressure loss below 20% in a sealed ampoule due to O_2 expenditure displays a knee. This knee is associated with process transition from kinetic order one to kinetic order zero at the initial and developed stages with the boundary defined by absorption of 0.8 - 1.2 O_2 mol/base-mol. Similar phenomenon at thermal oxidation of arylaliphatic polybenzoxazole was interpreted [3, p. 104] as a two-stage consecutive oxidation of aliphatic and aromatic and heterocyclic fragments, i.e. quick expenditure of higher oxidizing aliphatic structures defines clearly expressed kinetics of the initial stage of the process.

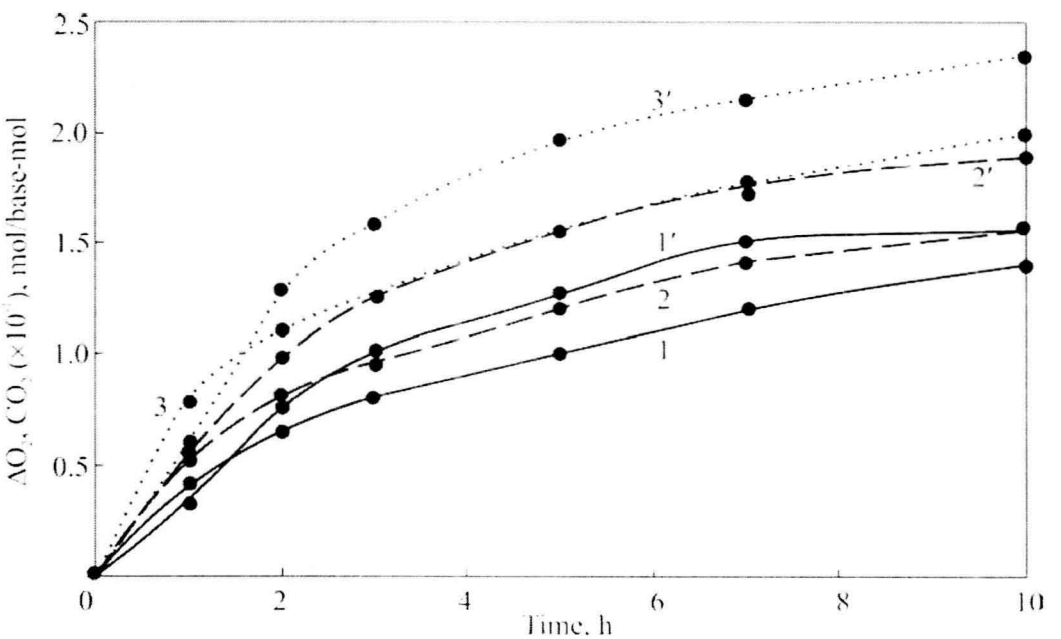

Figure 2. Kinetics of O_2 absorption (1 – 3) and CO_2 release (1' – 3') at PSF thermal oxidation in air at 300°C (1, 1'), 320°C (2, 2') and 350°C (3, 3')

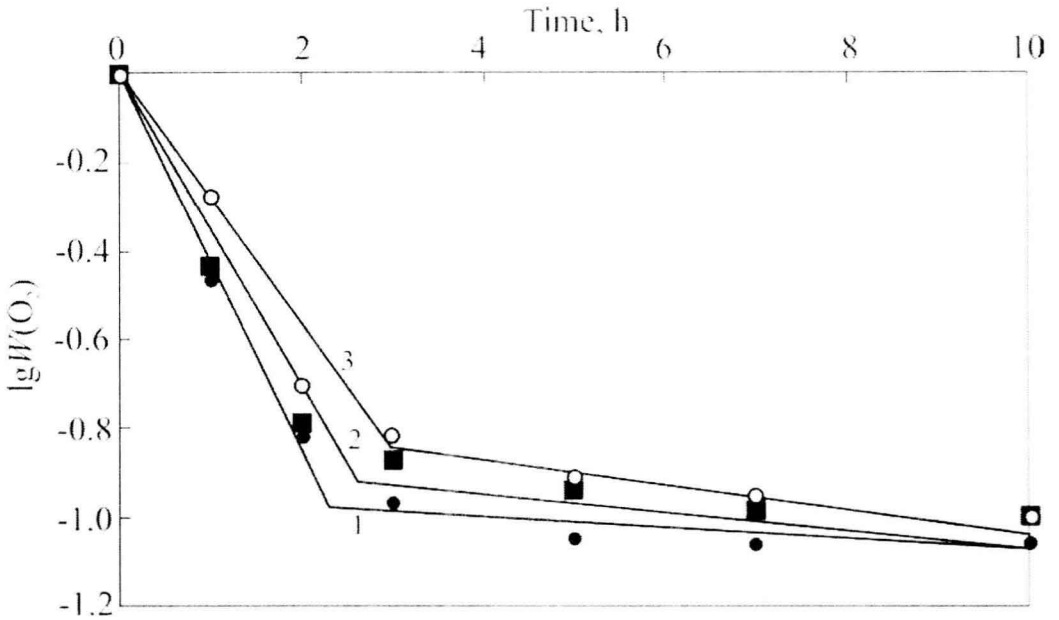

Figure 3. Time dependence anamorphism for PSF oxidation rate at 300°C (1), 320°C (2) and 350°C (3)

Kinetics changes with O_2 pressure (Figure 4). For processes proceeding under low pressure, sigmoid-shaped kinetic curves typical of P_{O_2} above 200 – 230 kPa (partial O_2 pressure in air) are transformed to S-shaped ones, and the induction period occurs not only in absorption kinetic, but also in gel accumulation. The dependence of initial O_2 absorption rates on the initial partial pressure of oxygen is approximately described by the following empirical equation:

$$V = P_{O_2}^{1/2}.$$

Such dependence may be caused by two reasons. The first is that the reaction proceeds in diffusion mode. This suggestion is rejected due to independence of specific O_2 absorption rates on PSF weighing (10 – 100 mg). As a consequence, kinetic dependence on P_{O_2} is inherent to the process mechanism.

It is known that hydrocarbon liquid oxidation kinetics in the absence of diffusion hindrances is independent of P_{O_2} [4, p. 119]. Oxidation of carbochain polymers in solution is also independent of P_{O_2} [5, p. 132]. However, for low-temperature oxidation of solid polyolefins this dependence is associated with O_2 participation in oxidation initiation at hydroperoxide decay. It is suggested [5, p. 134] that the part of block hydroperoxides decaying faster that single hydroperoxides increases with P_{O_2}. Another contribution is associated with relatively low (compared with the liquid phase) rate of alkyl macroradical reaction with O_2 even in the kinetic zone. This leads to a competition between chain termination reactions which causes changes in the composition of hydroperoxides [5, p. 136].

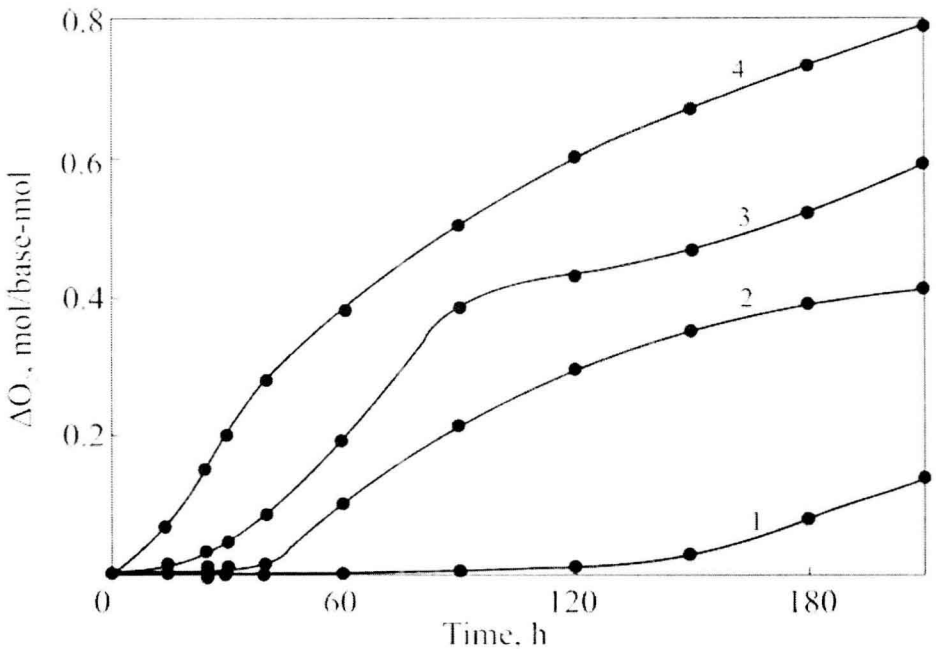

Figure 4. Kinetic curves of O_2 absorption by PSF at 320°C and O_2 pressure of 26.6 (1), 66.5 (2), 133.3 (3) and 399.9 kPa (4)

Anyway, autooxidation rates at low temperatures are associated with hydroperoxides. Hydroperoxides were not detected at high-temperature PSF oxidation. This may be explained taking into account their thermal instability. Another idea about oxidation rate independence of P_{O_2} occurred during studying high-temperature (270 - 360°C) PE oxidation [3, p. 101]. It is suggested that nearly linear dependence of V_{O_2} on P_{O_2} for PE at 300 - 360°C is associated with significant contribution of peroxy macroradical decomposition with formation of low-molecular mobile $OH^{\cdot}$ radical.

Besides the kinetics dependence on P_{O_2}, of special attention in PSF thermal oxidation is its self-excited accelerated type at P_{O_2} below 133.3 kPa. The time interval of autocatalysis at temperatures below 300°C is tens of minutes long (Figure 2). Therefore, autocatalysis may not be associated with branching products of low-temperature autooxidation, which are hydroperoxides, not accumulated at PSF high-temperature oxidation. As P_{O_2} changes, kinetic curves of O_2 absorption by PSF transform from S-shape to sigmoid. This phenomenon has no analogy in the literature (for example, σ-shape of PE oxidation kinetic curves at 240 - 300°C is also preserved at low P_{O_2} [2]). However, similar transformation was observed for oxidation kinetics ($H_2^+ + O_2$) at 485°C and various initial pressures [6, p. 106], i.e. in well-studied radical-chain, branched process. For high-temperature oxidation of polymers, it is suggested [3, p. 107] that self-excited accelerated type of reaction is associated with degenerated chain branching. Though the origin of intermediate branching products is not clear yet, by analogy with hydrocarbon oxidation in the gas phase the so-called "aldehyde

branching" is suggested, but the existence of different, not yet defined alternatives also accepted.

Thus, comparison of PSF high-temperature oxidation phenomenology with examples from the literature indicates the signs of radical-chain, apparently branched process.

PSF thermal oxidation in melt causes quick gel formation and yellowing (Figure 5). Gel formation kinetics at high P_{O_2} at the initial stages obeys the order one law with the activation energy E_a = (49 ± 15) kJ/mol. Besides the proximity of kinetic parameters - $E_a(\Delta O_2)$ = 72 kJ/mol and symbate property of corresponded curves shown in Figures 5 and 6, possessing $\Delta G = 0.09\Delta O_2$, the interrelation of oxidation and gel formation is outlined by dependence of the latter on P_{O_2}: P_{O_2} decrease to 26.6 kPa causes occurrence of the induction period in gel-fraction accumulation kinetics. Analogous dependence is also observed for PSF yellowing (Figure 5).

Gel formation and yellowing are the effective result of macromolecule size change and accumulation of functional groups in them. Before considering these processes separately, let us find a correlation between thermal processes in PSF at O_2 free access and standard tests in IIRT chamber, simulating polymer processing. As shown by this index (Figures 1 and 5), PSF degradation kinetics in IIRT chamber is adequate to thermal oxidation with free access of oxygen at partial pressure of 26.6 kPa. Under these conditions, gel formation points also approximately coincide. As contribution of PSF mechanical degradation is insignificant at shear stresses realized in IIRT, it is desirable to simulate processing by heating PSF up at P_{O_2} = 26.6 kPa.

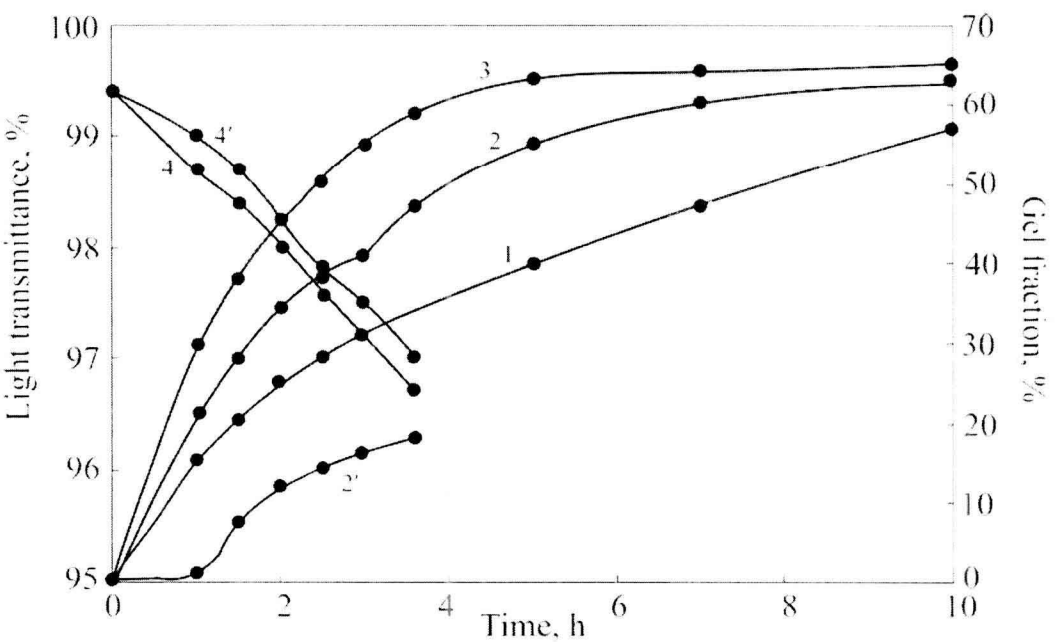

Figure 5. Kinetics of gel-fraction accumulation (1 – 3) and yellowing (4, 4') of PSF at 300°C (1), 320 °C (2, 2', 4, 4') and 350°C (3). Oxygen pressure: 212.8 (1 - 4) and 26.6 kPa (2', 4')

As PSF is heated up at free access of oxygen with P_{O_2} = 26.6 kPa and exposure durations limited by the gel formation point (3 h), a constant shift of MMD curve towards greater masses and simultaneous broadening are observed (Figure 6). All MMD moments subsequently increase during PSF free thermal oxidation (Figure 5). Such curve shape nearly corresponds to the initial stage of MMD change only in PSF tests in IIRT cylinder (Figure 1), when some decrease of molecular masses is observed after initial rise, except for tests at 300°C, where all MMD moments increase. By kinetic curve shape (but not by absolute changes) PSF behavior in the cylinder is similar to free degradation in the absence of oxygen (Figure 1). For long stay in IIRT it may be simulated as follows. From positions of dissolved O_2 presence in the polymer, conditions in IIRT represent a superposition of controllable presence or absence of O_2. As polymer melts, it still contacts O_2 residues located in a gap between the nozzle and the piston free from polymer. No external air is delivered. The process develops as thermal oxidation with O_2 deficiency (i.e. like with P_{O_2} = 26.6 kPa) until all O_2 in the system is spent. When O_2 resource is exhausted, the process transits from thermal oxidation to pure thermal reaction, for which kinetics of PSF molecular mass change is studied well. In case of thermolysis in vacuum at 380°C, degradation dominates over crosslinking. The first phase corresponds to real processing; in this phase melted PSF interacts with O_2 dissolved in it and O_2 gas residues, i.e. it oxidizes.

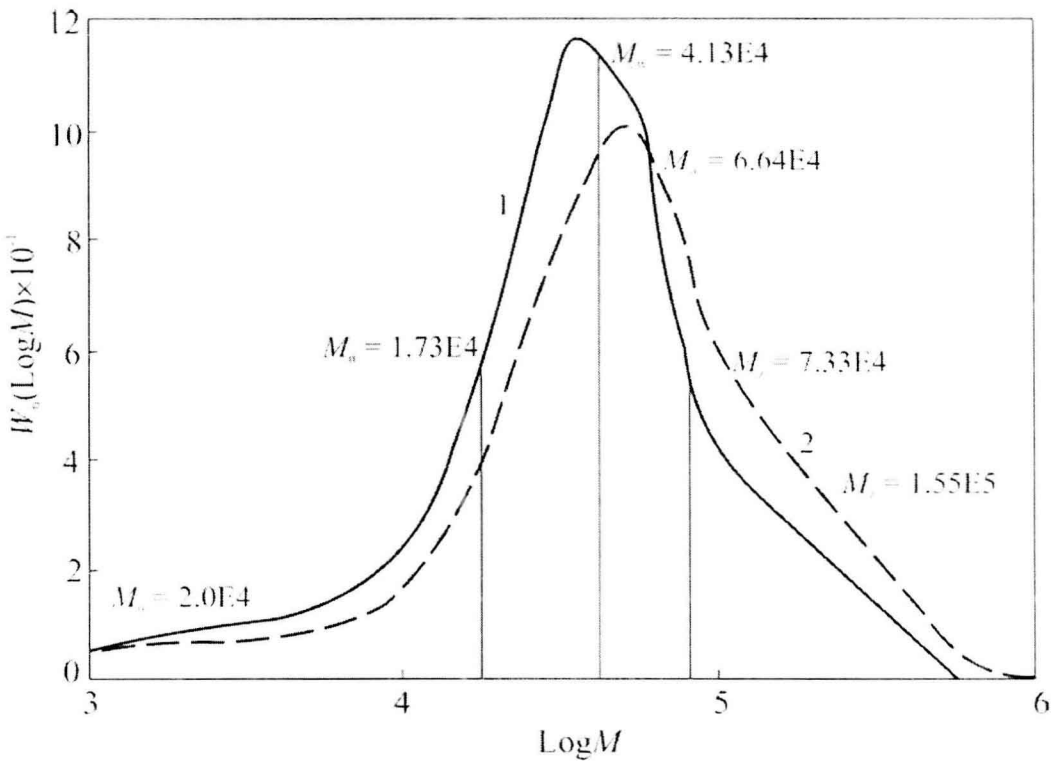

Figure 6. MMD for PSF before (1) and after (2) thermal oxidation during 1 h at 320°C

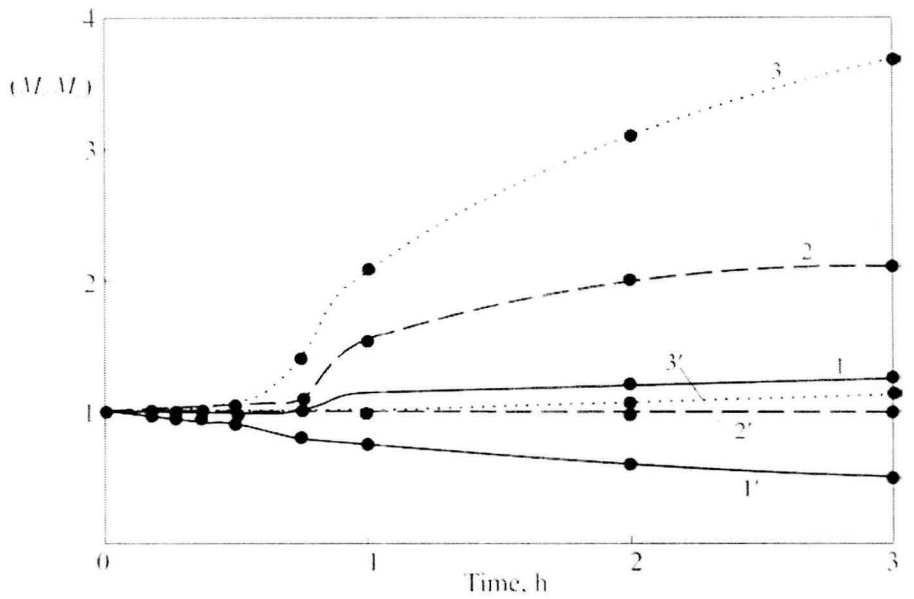

Figure 7. Relative change of PSF molecular mass during thermal oxidation at 320°C with P_{O_2} = 26.6 kPa (1 – 3) and in vacuum (1' – 3'); M_n (1, 1'), M_w (2, 2'), M_z (3, 3')

PSF molecular mass increases during thermal oxidation due to branching. A combination of viscosity gage and any other detector "on-line" gel chromatographer and the use of computer calculation in the framework of Zimm-Stockmayer theory made analysis of polymer branching much simpler. The method is designed to solve the reverse task – "adjustment" of experimental characteristic viscosity (viscosity gage) and its calculated value, obtained from MMD data from the neighboring "on-line" detector. To analyze the branching degree, one should know the so-called g factor, which is the relation of square radii of coils from analyzed and linear polymers. This factor is calculated by the relation of characteristic viscosities of branched and linear polymers with equal molecular masses. The factor is determined by direct file comparison for linear and branched polymers. The information is presented as a function

$$g = f(M)$$

and the number of branchings per molecule, B_n, calculated from the Zimm-Stockmayer equation in the frame work of statistical model as follows:

$$g = \left[1 + \frac{B_n}{\sqrt{7}} + \frac{4B_n}{9}\right]^{0.5}$$

and branching frequency

$$\lambda(M) = P \cdot \frac{B_n}{M},$$

where P is the repeating unit of the molecule, for example, monomeric unit, and the average branching frequency:

$$\overline{\lambda} = \frac{\sum c_i \lambda_i}{\sum c_i}.$$

Data in Figure 8 illustrate the branching increase during PSF thermal oxidation, which initially is the linear polymer (g = 1). The g function indicates regular increase of the branching degree with molecular mass. The branching frequency averaged by MMD $\left(\overline{\lambda} = \frac{\sum c_i \lambda_i}{\sum c_i}\right)$ increase linearly first with exposure and, finally, reaches the border value (0.25 branchings per base-mole) near the gel formation point (Figure 9). Therefore, branching, as well as molecular mass increase, happens during the induction period of O_2 absorption (Figure 4). The average inter-crosspoint distance M_c equals 4,000 – 5,000. According to the long-chain model, this is also the length of side chains. Temperature increase speeds up the branching process in PSF due to thermal oxidative degradation. The gel formation point at 340°C shifts to 1.5 h; $\overline{\lambda}$ increase is accelerated, simultaneously, for example, this index for 1 h exposure equals 0.36.

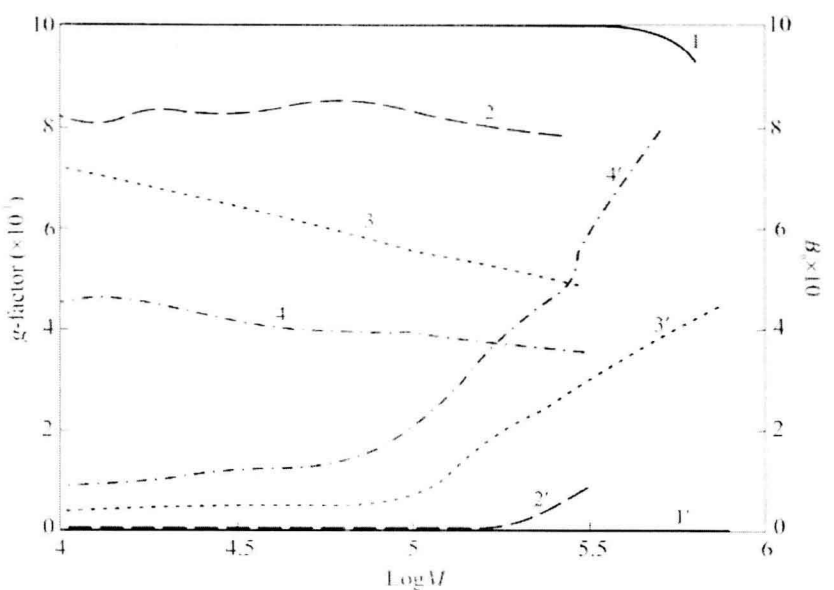

Figure 8. The effect of thermal oxidation (320°C, $P(O_2)$ = 26.6 kPa) on PSF branching indices: g-factor (1 – 4) and B_n^2 (1' – 4') at exposures of 0 (1, 1'), 0.5 (2, 2'), 1 (3, 3'), and 3 (4, 4') hours